



# Optical Characteristics of Overstressed Nanosecond Discharge Plasma Between An Electrode of Aluminum And Chalcopyrite ( $\text{CuInSe}_2$ ) In Argon, Nitrogen And Atmospheric Pressure Air

Alexander Shuaibov and Antonina Malinina

DVNZ "Uzhgorod National University"; Narodna pl. 3, Uzhgorod, Ukraine

## Correspondence

Antonina Malinina

DVNZ "Uzhgorod National University",  
Narodna pl. 3, Uzhgorod, Ukraine

E-mail: alexsander.shuaibov@uzhnu.edu.ua

- Received Date: 01 Sep 2021
- Accepted Date: 06 Sep 2021
- Publication Date: 09 Sep 2021

## Keywords

overstressed nanosecond discharge, aluminum, chalcopyrite, copper, indium, selenium, argon, nitrogen, air

## Copyright

© 2021 Science Excel. This is an open-access article distributed under the terms of the Creative Commons Attribution 4.0 International license.

## Abstract

The optical characteristics and parameters of an overstressed discharge of nanosecond duration between an aluminum electrode and an electrode from chalcopyrite ( $\text{CuInSe}_2$ ) in argon, nitrogen, and air at atmospheric pressure are presented. Due to microexplosions of natural inhomogeneities on the working surfaces of electrodes in a strong electric field, both aluminum and ternary chalcopyrite vapors are introduced into the plasma, which creates the prerequisites for the synthesis of thin films of quaternary chalcopyrite ( $\text{CuAlInSe}_2$ ) outside the discharge. The pulses of voltage and current across the discharge gap of  $d = 1$  mm and the pulsed energy contribution to the plasma are investigated. The plasma emission spectra were thoroughly studied, which made it possible to establish the main decay products of the chalcopyrite molecule and the energy states of atoms and singly charged ions of aluminum, copper and indium, which are formed in the discharge. Reference spectral lines of atoms and ions of aluminum, copper and indium have been revealed, which can be used to monitor the process of deposition of thin films of quaternary chalcopyrite in real time.

The transmission spectra of radiation synthesized in the experiment by thin films, which include aluminum, copper, indium and selenium, which are components of the quaternary chalcopyrite  $\text{CuAlInSe}_2$ , are presented.

## Introduction

The topic of research in the physics and technology of overstressed nanosecond discharges in molecular and atomic gases, which were ignited in the "needle-plane" and "needle-needle" electrode systems, continues to develop intensively [1-3], and the discharges themselves are used in various gas-discharge technologies in micro-nanoelectronics [4-6].

Plasma of high-current overstressed discharges in gases in most cases contains electrode materials [7-9], which can be used to synthesize the corresponding thin films on a dielectric substrate installed outside the discharge region [2,3]. Therefore, it is important for such discharges to conduct a thorough study of their characteristics and parameters, since the properties of the synthesized thin films depend on them.

The main characteristics of a spark discharge with a duration of 25-70 ns in air at atmospheric pressure are given in [10]. The discharge was ignited between two cylindrical electrodes made of brass or stainless steel, 6 mm in diameter and end

surfaces with a curvature radius of 3 mm at an interelectrode distance  $d = 0.1-15$  mm (pulse duration  $\tau = 25$  and 65-70 ns;  $U = 18$  kV). The spectral composition of plasma emission was determined mainly by the radiation of the products of erosion of the electrode material. Thus, in the spectrum of plasma emission based on brass vapors, the main radiation was concentrated in the spectral range of 200-230 nm; the identification of the spectrum and the nature of its emitters were not given in [10].

The results of studying the optical characteristics of an overstressed discharge of nanosecond duration between aluminum electrodes ( $d = 2$  and 6 mm) in nitrogen are presented in [11]. In the gap between the electrodes with a distance of  $d = 2$  mm, near the apex of the cathode, colored mini-jets of plasma based on aluminum vapor plasma were observed, and the most intense spectral lines Al I and Al II: 396.4 were observed in the plasma emission spectra; 396.12 nm; 622.62; 623.17; 704.21; 705.66; 706.36, respectively. The luminescence duration at the Al I and Al II transitions prevailed 2  $\mu\text{s}$ , which is longer than the duration of the current pulses; therefore, the authors of [11] assumed the recombination

**Citation:** Shuaibov A, Malinina A. Optical characteristics of overstressed nanosecond discharge plasma between an electrode of aluminum and chalcopyrite ( $\text{CuInSe}_2$ ) in argon, nitrogen and atmospheric pressure air. Biomed Transl Sci. 2021; 1(3):1-10.

nature of the plasma glow at the Al and Al II transitions.

The results of a study of UV radiation from a high-voltage pulsed multielectrode discharge in air at atmospheric pressure are presented in [12]. A nanosecond discharge was ignited in the form of a set of successive microplasma formations with a specific energy contribution at the level of  $1 \text{ kJ} / \text{cm}^3$ , an electron concentration of  $10^{17} \text{ cm}^{-3}$  and an energy, introduced into the discharge of  $\sim 200 \text{ MJ}$ . In the plasma emission, the radiation of atoms and ions of the material of the electrodes made of copper or stainless steel dominated.

In addition to the aluminum plasma, vapors and other metals (copper, iron, etc.) were introduced into the discharge gap of overstressed discharges of nanosecond duration ( $p = 101 \text{ kPa}$ ) [12,13]. At an interelectrode distance  $d = 3 \text{ mm}$  and pressures of air, nitrogen, or argon 30 50 100 Torr, a runaway electron beam is formed in the plasma of this type of discharge. Blue jets were generated when the cathode was made of stainless steel. Green jets were generated for a copper cathode at gas pressures of 30 and 50 Torr. For the aluminum cathode, the jets were blue. The appearance of these plasma jets is caused by explosions of microinhomogeneities on the surface of electrodes and electroerosion of the metal, as a result of which flows of metal vapors are formed, which filled the discharge gap [14].

A research of the emission spectra of a nanosecond discharge in nitrogen at pressures of 100-200 Torr showed that the plasma from the central part of the discharge gap emits only intense bands of the nitrogen molecule. For a contracted discharge in air at  $p = 200 \text{ Torr}$ , the emission spectrum recorded a characteristic broadband continuum in the wavelength range 200-800 nm, spectral lines of atomic nitrogen ions (N II), oxygen atom lines and NO radical bands [12]. From the plasma in the vicinity of the cathode tip, the emission of Al I, Fe I atoms and FeII ions predominated.

In [15], the results of a study of thin-film solar cells  $\text{CuIn}_{1-x}\text{Al}_x\text{Se}_2$  (CIASe), which were prepared on the basis of a sequential process of selenization of metal precursors, are presented. Polycrystalline CIAS thin films with a chalcopyrite structure were synthesized. The best solar cells based on CIASe have an efficiency of 6.5%, with an Aluminum / (Indium + Aluminum) ratio of 0.2. Comparison of these values with similar data for a device without aluminum showed a significant increase in their efficiency due to an increase in the energy gap of the absorber in quaternary compounds of the  $\text{CuIn}_{1-x}\text{Al}_x\text{Se}_2$  type and better matching of the solar radiation spectrum in the infrared wavelength range with the absorption spectrum of the quaternary chalcopyrite.

Therefore, the development of new gas-discharge methods for the synthesis of thin films based on complex chalcopyrites of the  $\text{CuIn}_{1-x}\text{Al}_x\text{Se}_2$  type is of considerable practical interest for use in photovoltaic devices.

The results of an experimental study of the optical characteristics of the plasma of an overstressed discharge of nanosecond duration between an aluminum electrode and an electrode from chalcopyrite in argon, nitrogen at atmospheric pressure are presented in the article. Based on the electrode sputtering products, thin films were synthesized from the vapor of ternary chalcopyrite and the products of its destruction in plasma and aluminum, and their transmission spectra were studied.

## Technique and experimental conditions

An intense nanosecond discharge between an aluminum electrode and an electrode from chalcopyrite ( $\text{CuInSe}_2$ ) was ignited in a vacuum discharge chamber made of dielectric. A diagram of the discharge chamber with a system of electrodes and a device for the deposition of thin films is shown in figure. 1. The distance between the electrodes is  $\sim 1 \text{ mm}$ . The discharge chamber was evacuated with a foreline pump to a residual air pressure of 10 Pa, and then buffer gases were filled into the chamber: argon, nitrogen, or air to a pressure of 101 kPa. The diameter of the cylindrical electrodes is 5 mm. The radius of curvature of the working end surface of the electrodes is  $\sim 3 \text{ mm}$ .

The discharge in atmospheric pressure buffer gases was initiated using a high-voltage modulator of voltage pulses with a total duration of 50-150 ns and an amplitude of positive and negative components of 20-40 kV. The repetition rate of voltage pulses is 100 Hz. Oscillograms of voltage pulses across the discharge gap and oscillograms of current pulses were recorded using a broadband capacitive voltage divider, a Rogowski coil, and a 6LOR-04 broadband oscilloscope with a time resolution of 1-2 ns.

An MDR-2 monochromator and a photomultiplier (FEU-106) were used to record the plasma emission spectra. The signal from the photomultiplier was fed to an amplifier and was recorded using an amplitude-digital converter in an automated system for measuring spectra on a personal computer display. The discharge radiation was investigated in the spectral range of 200-650 nm.

The control experimental findings in gases of atmospheric pressure, which were carried out with a discharge between two electrodes made of chalcopyrite and two aluminum electrodes, are presented in [3,16]. The interelectrode distance in all cases was 1 mm, which made it possible to achieve a significant overstress in the discharge gap. The discharge visually looked as spatially homogeneous, which may be due to the ionization of the gaseous medium from the beam of runaway electrons and the accompanying X-ray radiation [17]. The plasma volume depended on the voltage pulse repetition rate. The "point discharge" mode was obtained only at voltage pulse repetition rates in the range  $f = 40\text{-}100 \text{ Hz}$ . With an increase in the frequency to 1000 Hz, the volume of the plasma of the gas-discharge emitter grew from 10 to  $100 \text{ mm}^3$ , however, operation in this mode could only be short-term due to the strong heating of the discharge device.

Typical oscillograms of voltage and current pulses in discharges between two chalcopyrite and aluminum electrodes are given in [3,16]. Voltage and current oscillograms were in the form of oscillations decaying in time with a duration of about 7-10 ns, which is due to the mismatch of the output resistance of the high-voltage modulator with the load resistance. The maximum voltage amplitude reached 40-60 kV, and the current amplitude was 120-150 A (electrodes from chalcopyrite). For an overstressed discharge of nanosecond duration between aluminum electrodes ( $d = 1 \text{ mm}$ ) in argon at atmospheric pressure, the maximum voltage oscillations reached 35-40 kV, and current up to 250 A.

Figures 2 and 3 show the pulsed discharge power in argon between two electrodes from chalcopyrite, as well as between

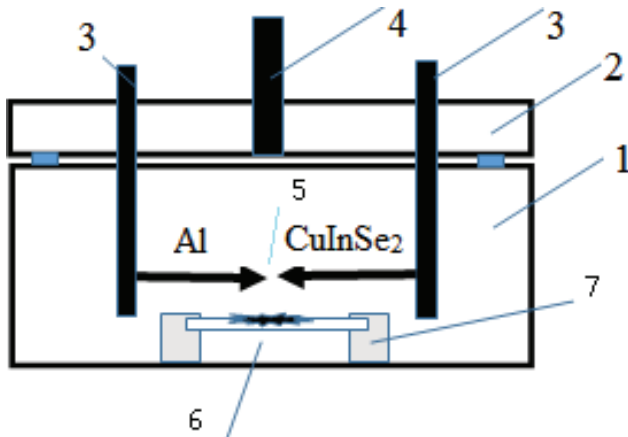


**Figure 1.** The scheme of the discharge device for the synthesis of chalcopyrite thin films on the surface of glass or quartz: 1 - a plexiglas discharge chamber, 2 - an upper flange, 3 - hermetic metal leads, 4 - a fitting for connecting to a vacuum gas mixing system, 5 - electrodes with Al and chalcopyrite, 6 - glass substrate with a film based on sputtered electrodes, 7 - plate fixing system.

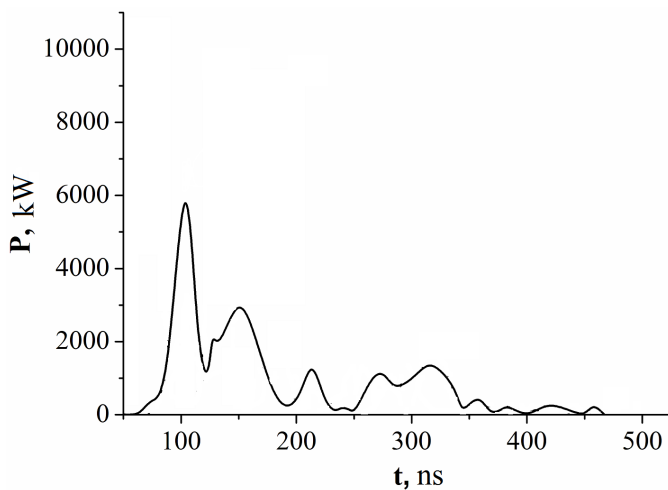


**Figure 2.** Pulsed power of overstressed discharge of nanosecond duration at  $p(\text{Ar}) = 101 \text{ kPa}$

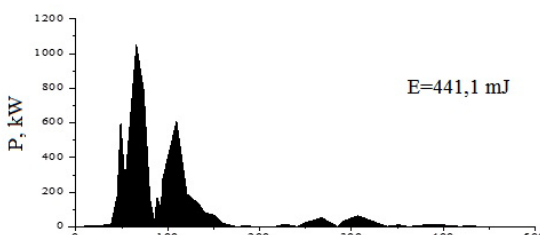


**Figure 3.** Pulsed power of overstressed discharge of nanosecond duration between aluminum electrodes ( $d = 1 \text{ mm}$ ) at:  $p(\text{Ar}) = 101 \text{ kPa}$ .

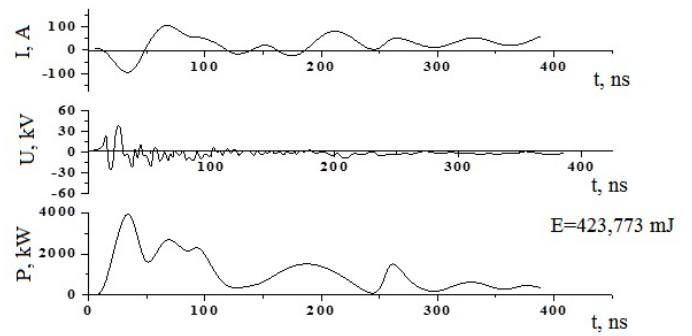


**Figure 4A.** Current, voltage and pulsed power oscillograms of overstressed discharge of nanosecond duration between electrodes made of aluminum and chalcopyrite  $\text{CuInSe}_2$  at an argon pressure of 101 kPa.

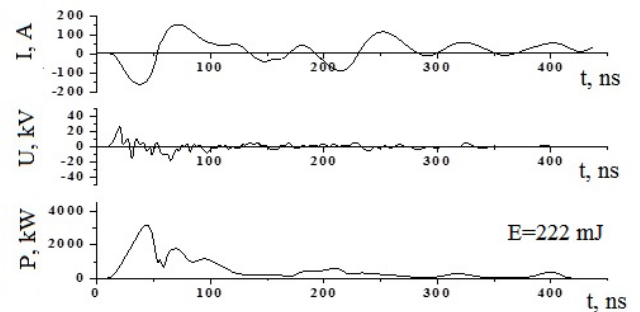


**Figure 4B.** Oscillograms of current, voltage and pulsed power of overstressed bipolar nanosecond discharge between aluminum and chalcopyrite electrodes ( $\text{CuInSe}_2$ ) at an air pressure of 101 kPa.

two aluminum electrodes ( $d = 1 \text{ mm}$ ;  $p(\text{Argon}) = 101 \text{ kPa}$ ). The main part of the pulsed electric power was introduced into the plasma during the first 150-200 ns and reached 5-6 MW (chalcopyrite electrodes).

Graphical integration of the pulsed power made it possible to determine the energy of one discharge pulse, which was introduced into the plasma. Thus, the energy contribution to the intense nanosecond discharge between chalcopyrite electrodes reached 400 mJ ( $p(\text{Argon}) = 101 \text{ kPa}$ ), and for a discharge between aluminum electrodes it was 441 J (Figure 3).

At  $p(\text{Argon}) = 101 \text{ kPa}$  (Fig. 4a), the maximum voltage amplitude swing was about 45 kV, and the duration of the main part of the voltage oscillogram was 100 ns. The maximum amplitude of the current pulse reached 180-200 A, and its total duration was 400-500 ns. It is likely that the diffuse discharge persisted only in the first 100-120 ns, and after that it passed into the contracted state. The maximum value of the pulsed power of the discharge was observed in the first 130 ns from the moment of its ignition and was equal to 4 MW. At an argon pressure of 101 kPa, the energy of an individual electrical pulse was 423 mJ (Figure 4). A decrease in the argon pressure to 13.3 kPa led to a decrease in the electric pulse energy of 46 mJ.

At an air pressure of 101 kPa, the maximum voltage amplitude swing was about 30 kV, and the duration of the main part of the voltage oscillogram was also 100 ns (Figure 4b). The

maximum amplitude of the current pulse reached 150 A, and its total duration was 400-450 ns (Figure 4b), the maximum value of the pulsed power of the discharge was observed in the first 40 ns from the moment of its ignition and was equal to 3.5 MW. The energy of an individual electrical pulse was 222 mJ (Figure 4b). Comparison of the time dependence of the pulsed power for a discharge in argon (Figure 4) and in air (Figure 4b) showed that in argon the pulsed power retains high values for 300 ns, and for a discharge in air this gap did not predominate 130 ns. This behavior of the pulsed power in time is due to the different resistances of argon and air to atmospheric pressure during the channel stage of the nanosecond discharge.

### Optical characteristics of plasma

Control studies of plasma emission spectra were carried out for overvoltages of a nanosecond discharge in argon between the aluminum electrodes; their results are presented in [16]. The emission spectra of the discharge plasma between the electrodes from the CuInSe<sub>2</sub> compound are shown in Fig. 5. When decoding the emission spectra of the discharge, reference books [18-20] were used.

Spectral lines of atoms, copper ions and indium atoms (lines 1-5; Figure 5) were observed against the background of continuous plasma emission. The nature of continuous plasma emission in argon can be associated with thermal or recombination radiation of plasma, in air or mixtures of nitrogen with oxygen with the radiation of alumina nanostructures. Copper and indium atoms are less bound in the chalcopyrite molecule, which is the main component of massive electrodes [21]; therefore, the linear part of the plasma emission spectrum is caused by separate spectral lines of atoms and singly charged ions of copper and indium, as for gas-discharge plasma based on air or nitrogen for overvoltages a nanosecond discharge of atmospheric pressure between copper electrodes [22]. The emission spectrum of the gaseous component, argon, was not manifested in this spectral region.

The second group of spectral lines (lines 6-15; Figure 5) was observed against the background of continuous low-intensity radiation, which grew weakly with increasing wavelength. Spectral lines (11-14) were represented by singly charged argon ions, while other lines belonged to copper and indium atoms. Radiation in the spectral range of 460-630 nm looked like molecular bands, against the background of which separate low-intensity spectral lines of atoms and ions of argon and selenium were observed.

Plasma emission, represented by spectral lines of low intensity (16-31), which were observed against the background of a continuum growing in intensity, is associated with the radiative decay of excited atoms and singly charged argon ions. Emission of metals in this spectral range was represented by spectral lines: 402.26; 484.22; 515.83 nm Cu I and 451.13 nm In I.

At an argon pressure of 101 kPa, in the spectrum of plasma emission based on a mixture of aluminum and chalcopyrite vapors, the shortest-wavelength and most intense part of the spectrum (lines 1-10) was represented by the spectral lines of atoms and singly charged ions of copper and aluminum. The spectral lines were closely located in the background of the continuum and actually formed a certain band with a base length of 50 nm (from 200 to 250 nm).

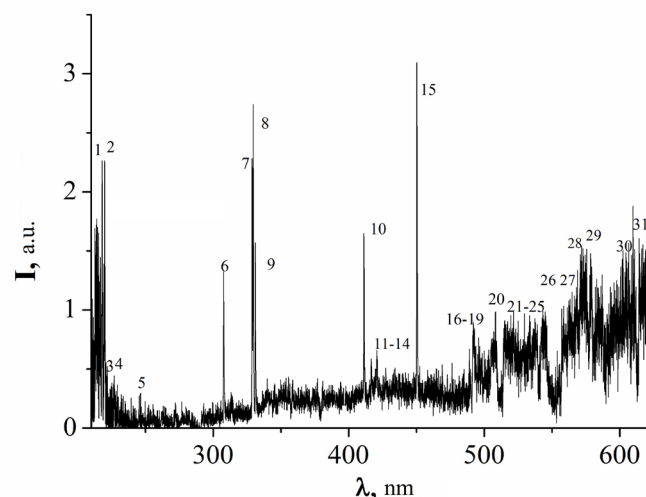


**Figure 5.** The spectrum of plasma emission of the overstressed discharge of nanosecond duration between the electrodes of chalcopyrite at  $p(\text{Argon}) = 101 \text{ kPa}$ .

The second group of spectral lines, which were also observed against the background of continuous radiation in the spectral range of 308-451 nm, had a higher degree of separation, but their intensities were low. In addition to atoms and singly charged ions of copper and aluminum, separate lines of Ar I, Ar II were also observed in the violet and blue regions of the spectrum. Only the atomic spectral lines 410.17 and 451.13 nm of In I appeared in the emission from indium lines.

In the spectral range of 450-650 nm, the intensity of continuous radiation increased strongly with increasing radiation wavelength. Against the background of continuous radiation, mainly the spectral lines of the argon and copper atoms were observed. The main reason for the appearance of an intense continuum in the spectrum is the transition of the diffuse form of an overstressed discharge of nanosecond duration into a contracted state (spark) at atmospheric pressure of argon.

A decrease in the argon pressure to 13.3 kPa promoted the ignition of the discharge in a diffuse form, and the contraction was significantly reduced. This led to a better manifestation in the emission of individual spectral lines of atoms and singly charged ions of copper, aluminum and argon

In the plasma emission spectra of vapor-gas mixtures based on aluminum, chalcopyrite and nitrogen molecules, as well as the products of their dissociation, the radiation of an overstressed discharge of nanosecond duration in the spectral range of 200-240 nm consisted of a group of closely located spectral lines of an atom and a singly charged copper ion, as well as lines of an atom and a singly charged aluminum ion (Table 2). The spectral lines of copper were similar to those found in the emission spectra of an overstressed discharge of nanosecond duration between copper or chalcopyrite electrodes in atmospheric pressure air at a distance between the copper electrodes  $d = 1, 2 \text{ mm}$  [2,3], but they were placed against a background of continuous radiation, whose shape was different from the continuum for a discharge in an argon mixture (Figure 6). For a discharge in gas-vapor mixtures containing oxygen (air or nitrogen of "technical" purity), we

**Table 1.** The results of identification of the most intense spectral lines of the atom and single-charged aluminum ion, as well as the molecular bands of the decay products of the chalcopyrite molecule in the overstressed discharge of nanosecond duration at  $p(\text{Ar}) = 101.3 \text{ kPa}$ .

№	$\lambda_{\text{tabl.}}$ , nm	$I_{\text{exp.}}$ , a.u.	Object	$E_{\text{low.}}$ , eV	$E_{\text{up.}}$ , eV	Lower <sub>term</sub>	Upper <sub>term</sub>
1	214.89	3.90	Cu I	1.39	7.18	4s <sup>2</sup> 2D	5f <sup>2</sup> F <sup>o</sup>
2	218.17	3.94	Cu I	0.00	5.68	4s <sup>2</sup> S	4p' <sup>2</sup> P <sup>o</sup>
3	219.56	3.29	Cu II	8.78	14.43	4p <sup>3</sup> D <sup>o</sup>	4d <sup>3</sup> F
4	219.95	2.88	Cu I	1.39	7.02	4s <sup>2</sup> 2D	4p'' <sup>2</sup> D <sup>o</sup>
5	221.45	2.40	Cu I	1.39	6.98	4s <sup>2</sup> 2D	4p'' <sup>2</sup> P <sup>o</sup>
6	224.20	2.45	Cu II	3.0	8.49	4p	3D
7	239.07	1.07	Al II	13.07	18.26	4p <sup>3</sup> P <sup>o</sup>	10d <sup>3</sup> D
8	261.83	0.79	Cu I	1.39	6.12	4s <sup>2</sup> 2D	5p <sup>2</sup> P <sup>o</sup>
9	284.02	0.68	Al I	4.02	8.39	3d <sup>2</sup> D	3d <sup>2</sup> D <sup>o</sup>
10	306.34	0.92	Cu I	1.64	5.68	4s2 2D	4p' <sup>2</sup> P <sup>o</sup>
11	308.21	1.34	Al I	0.00	4.02	3p <sup>2</sup> P <sup>o</sup>	3d <sup>2</sup> D
12	309.27	1.88	Al I	0.01	4.02	3p <sup>2</sup> P <sup>o</sup>	3d <sup>2</sup> D
13	324.75	1.42	Cu I	0	3.82	4s <sup>2</sup> S	4p <sup>2</sup> P <sup>o</sup>
14	327.39	1.43	Cu I	0	3.39	4s <sup>2</sup> S	4p <sup>2</sup> P <sup>o</sup>
15	329.05	1.05	Cu I	5.07	8.84	4p' <sup>4</sup> F <sup>o</sup>	4d' <sup>4</sup> F
16	360.65	0.97	Ar I	11.62	15.06	4s [ 1/2 ] <sup>o</sup>	6p [ 1/2 ]
17	394.40	1.27	Al I	0.00	3.14	3p <sup>2</sup> P <sup>o</sup>	4s <sup>2</sup> S
18	396.15	1.76	Al I	0.01	3.14	3p <sup>2</sup> P <sup>o</sup>	4s <sup>2</sup> S
19	402.26	0.64	Cu I	3.79	6.87	4p <sup>2</sup> P <sup>o</sup>	5d <sup>2</sup> D
20	405.67	0.70	Al II	15.47	18.52	3s4d <sup>1</sup> D	3s15p <sup>1</sup> P0
21	410.17	1.19	In I	-	3.02	5s <sup>2</sup> 5p <sup>2</sup> P <sup>o</sup>	5s <sup>2</sup> 6s <sup>2</sup> S1/2
22	415.85	1.18	Ar I	11.55	14.53	4s [ 1/2 ] <sup>o</sup>	5p [ 1 1/2 ]
23	417.83	1.12	Ar II	16.64	19.61	4s 4P	4p 4D0
24	419.07	0.74	Ar I	11.55	14.51	4s [ 1/2 ] <sup>o</sup>	5p [ 2 1/2 ]
25	420.06	0.90	Ar I	11.55	14.50	4s [ 1/2 ] <sup>o</sup>	5p [ 2 1/2 ]
26	422.26	1.22	Ar II	19.87	22.80	4p <sup>2</sup> P <sup>o</sup>	5s <sup>2</sup> P
27	425.93	0.73	Ar I	11.83	14.74	4s' [ 1/2 ] <sup>o</sup>	5p' [ 1/2 ]
28	426.62	0.70	Ar I	11.62	14.53	4s [ 1/2 ] <sup>o</sup>	5p [ 1 1/2 ]
29	427.21	0.76	Ar I	11.62	14.52	4s [ 1/2 ] <sup>o</sup>	5p [ 1 1/2 ]
30	430.01	0.76	Ar I	11.62	14.51	4s' [ 1/2 ] <sup>o</sup>	5p [ 2 1/2 ]
31	433.35	0.89	Ar I	11.83	14.69	4s' [ 1/2 ] <sup>o</sup>	5p' [ 1 1/2 ]
32	451.13	1.65	In I	0.27	3.02	5s <sup>2</sup> 5p <sup>2</sup> P <sup>o</sup>	5s <sup>2</sup> 6s <sup>2</sup> S1/2
33	484.22	1.18	Cu I	5.24	7.80	4p' <sup>4</sup> F <sup>o</sup>	5s' <sup>4</sup> D
34	515.83	1.32	Cu I	5.69	8.09	4p' <sup>2</sup> P <sup>o</sup>	5s' <sup>2</sup> D
35	516.22	1.13	Ar I	12.91	15.31	4p [ 1/2 ]	6d [ 1/2 ] <sup>o</sup>
36	518.77	1.42	Ar I	12.91	15.30	4p [ 1/2 ]	5d' [ 1 1/2 ] <sup>o</sup>
37	549.58	1.57	Ar I	13.08	15.33	4p [ 2 1/2 ]	6d [ 3 1/2 ] <sup>o</sup>
38	555.87	1.46	Ar I	12.91	15.14	4p [ 1/2 ]	5d [ 1 1/2 ] <sup>o</sup>
39	556.69	1.45	Se II				
40	594.92	2.00	Ar I	13.28	15.35	4p' [ 1 1/2 ]	6d [ 1 1/2 ]
41	603.21	2.25	Ar I	13.08	15.13	4p [ 2 1/2 ]	5d [ 3 1/2 ] <sup>o</sup>

**Table 2.** The results of identification of the most intense spectral lines of the atom, single-charged aluminum ion and molecular bands of the decay products of the molecule chalcopyrite and nitrogen in an overstressed discharge of nanosecond duration ignited at a nitrogen pressure of 101 kPa.

№	$\lambda_{\text{tabl}}, \text{nm}$	$I_{\text{exp}}, \text{a.u.}$	Object	$E_{\text{low}}, \text{eV}$	$E_{\text{up}}, \text{eV}$	Lower <sub>term</sub>	Upper <sub>term</sub>
1	214.89	3.88	Cu I	1.39	7.18	4s <sup>2</sup> 2D	5f <sup>2</sup> F <sup>o</sup>
2	218.17	2.33	Cu I	0.00	5.68	4s <sup>2</sup> S	4p' <sup>2</sup> P <sup>o</sup>
3	219.56	3.41	Cu II	8.78	14.43	4p <sup>3</sup> D <sup>o</sup>	4d <sup>3</sup> F
4	219.95	2.32	Cu I	1.39	7.02	4s <sup>2</sup> 2D	4p'' <sup>2</sup> D <sup>o</sup>
5	221.45	2.34	Cu I	1.39	6.98	4s <sup>2</sup> 2D	4p'' <sup>2</sup> P <sup>o</sup>
6	225.80	2.5	Al I	0.00	5.49	3p <sup>2</sup> P <sup>o</sup>	7s <sup>2</sup> S
7	239.07	1.08	Al II	13.07	18.26	4p <sup>3</sup> P <sup>o</sup>	10d <sup>3</sup> D
8	261.83	0.92	Cu I	1.39	6.12	4s <sup>2</sup> 2D	5p <sup>2</sup> P <sup>o</sup>
9	284.02	1.66	Al I	4.02	8.39	3d <sup>2</sup> D	3d <sup>2</sup> D <sup>o</sup>
10	306.34	1.3	Cu I	1.64	5.68	4s <sup>2</sup> 2D	4p' <sup>2</sup> P <sup>o</sup>
11	308.21	1.59	Al I	0.00	4.02	3p <sup>2</sup> P <sup>o</sup>	3d <sup>2</sup> D
12	309.27	2.30	Al I	0.01	4.02	3p <sup>2</sup> P <sup>o</sup>	3d <sup>2</sup> D
13	313.60	0.86	N2	Second positive system C <sup>3</sup> Pu+-B <sup>3</sup> Pg+ (2;1)			
14	315.93	0.80	N2	Second positive system C <sup>3</sup> Pu+-B <sup>3</sup> Pg+ (1;0)			
15	324.75	2.6	Cu I	0	3.82	4s <sup>2</sup> S	4p <sup>2</sup> P <sup>o</sup>
16	327.39	2.38	Cu I	0	3.39	4s <sup>2</sup> S	4p <sup>2</sup> P <sup>o</sup>
17	329.05	2.03	Cu I	5.07	8.84	4p' <sup>4</sup> F <sup>o</sup>	4d' <sup>4</sup> F
18	337.13	1.27	N2	Second positive system C <sup>3</sup> Pu+-B <sup>3</sup> Pg+ (0;0)			
19	344.60	1.25	N2	Second positive system C <sup>3</sup> Pu+-B <sup>3</sup> Pg+ (4;5)			
20	353.67	0.73	N2	Second positive system C <sup>3</sup> Pu+-B <sup>3</sup> Pg+ (1;2)			
21	357.69	1.67	N2	Second positive system C <sup>3</sup> Pu+-B <sup>3</sup> Pg+ (0;1)			
22	371.05	0.77	N2	Second positive system C <sup>3</sup> Pu+-B <sup>3</sup> Pg+ (2;4)			
23	375.54	0.84	N2	Second positive system C <sup>3</sup> Pu+-B <sup>3</sup> Pg+ (1;3)			
24	380.49	0.71	N2	Second positive system C <sup>3</sup> Pu+-B <sup>3</sup> Pg+ (0;2)			
25	394.30	2.08	N2	Second positive system C <sup>3</sup> Pu+-B <sup>3</sup> Pg+ (2;5)			
26	394.40	2.57	Al I	0.00	3.14	3p <sup>2</sup> P <sup>o</sup>	4s <sup>2</sup> S
27	396.15	2.94	Al I	0.01	3.14	3p <sup>2</sup> P <sup>o</sup>	4s <sup>2</sup> S
28	402.26	1.95	Cu I	3.79	6.87	4p <sup>2</sup> P <sup>o</sup>	5d <sup>2</sup> D
29	405.67	1.78	Al II	15.47	18.52	3s4d <sup>1</sup> D	3s15p <sup>1</sup> P <sup>o</sup>
30	409.48	2.7	N2	Second positive system C <sup>3</sup> Pu+-B <sup>3</sup> Pg+ (4;8)			
31	410.17	1.4	In I	-	3.02	5s <sup>2</sup> 5p <sup>2</sup> P <sup>o</sup>	5s <sup>2</sup> 6s <sup>2</sup> S1/2
32	420.05	1.58	N2	Second positive system C <sup>3</sup> Pu+-B <sup>3</sup> Pg+ (2;6)			
33	423.65	1.85	N2	Second positive system C <sup>3</sup> Pu+-B <sup>3</sup> Pg+ (1;2)			
34	434.36	1.27	N2	Second positive system C <sup>3</sup> Pu+-B <sup>3</sup> Pg+ (0;4)			
35	441.67	2.18	N2	Second positive system C <sup>3</sup> Pu+-B <sup>3</sup> Pg+ (3;8)			
36	451.13	3.56	In I	0.27	3.02	5s <sup>2</sup> 5p <sup>2</sup> P <sup>o</sup>	5s26s <sup>2</sup> S1/2
37	459.97	2.76	N2	Second positive system C <sup>3</sup> Pu+-B <sup>3</sup> Pg+ (2;4)			
38	500.515	4.41	N II	25.50	27.97	3s <sup>5</sup> P	3p <sup>5</sup> P <sup>o</sup>
39	515.83	1.50	Cu I	5.69	8.09	4p' <sup>2</sup> P <sup>o</sup>	5s' <sup>2</sup> D
40	556.69	1.22	Se II				
41	566.66	2.9	N II	18.46	20.65	2s <sup>2</sup> 2p3s <sup>3</sup> P <sup>o</sup>	2s <sup>2</sup> 2p3p <sup>3</sup> D
42	618.86	2.66	Cu II	14.99	16.99	4p'' <sup>1</sup> D <sup>o</sup>	5d <sup>3</sup> F

recorded the radiation of nanostructures of aluminum oxide and UV and visible spectral range ( $\lambda\lambda = 200\text{-}640\text{ nm}$ ). A typical radiation spectrum of such a plasma of an overstressed discharge of nanosecond duration between aluminum electrodes in an oxygen-containing gas medium is shown in Figure 9.

In the emission spectra of the discharge on mixtures of air with impurities of aluminum vapors [16], broad emission bands were obtained with maxima in the spectral ranges of 410-420 nm and 300-390 nm (Figure 9). The highest radiation intensity of these bands is obtained at pressures of oxygen-containing gases of 100-200 kPa. In a discharge in argon-based mixtures, these bands were absent in the emission spectra of an overstressed discharge of nanosecond duration. In [23,24], the results of studying the cathodoluminescence spectra of nanostructured ceramics of aluminum oxide are presented. The spectrum of this cathodoluminescence was practically identical to the spectrum that was obtained in our study of the emission of an overstressed discharge of nanosecond duration at air pressures of 101-202 kPa or on a mixture of nitrogen with oxygen ( $p = 101\text{ kPa}$ ; Figure 9). In these spectra, the main was the emission band with a maximum at  $\lambda\lambda = 410\text{-}420\text{ nm}$  (photon energy 3.0 eV), which was adjacent to a wider short-wavelength band with maxima of the photon energy at  $E = 3.4$ ; 3.8; 4.3 eV. The ultraviolet photo- and cathodoluminescence bands of nanostructured aluminum oxide ceramics are associated with the radiation of  $F^+$  centers formed by oxygen vacancies [24,25].

A group of intense spectral lines and bands is located in the spectral range of 250-390 nm (Table 2). For this part of the spectrum, the most characteristic were the spectral lines of copper and aluminum atoms, as well as bright bands of the second positive system of the nitrogen molecule. Radiation of indium atoms in the visible region of wavelengths was represented by spectral lines 410.17; 451.13 nm In I. The characteristic spectral line with a wavelength of 500.5 nm N II, which is often observed in the emission spectra of nanosecond discharges in atmospheric pressure air, also appeared in the plasma emission spectrum [26]. The characteristic spectral lines of the copper atom in the visible range of the spectrum are 510.55; 515.83; 521.04; 556.69 nm Cu I, which were of low-intensity, in contrast to the case of an overstressed discharge of nanosecond duration plasma between copper electrodes in nitrogen or air, when there was an effective process of energy transfer from nitrogen molecules in metastable states to copper atoms [12,13].

In the red region of the spectrum, the intensity of the spectral line of the singly charged copper ion 618.86 nm Cu II was distinguished, the intensity of which almost doubled with an increase in the nitrogen pressure from 13.3 to 101 kPa.

In the yellow-red region in the spectrum of plasma emission (Figure 7), a continuum was recorded, the intensity of which increased with increasing wavelength in the range 550-665 nm, against the background of which individual spectral lines of low intensity and molecular bands were observed, which can be attributed to radiation selenium molecules and products of their dissociation in the discharge plasma.

The density of electrons in discharges with an explosive (ectonic) mechanism for introducing vapors of the electrode material at atmospheric pressures of a buffer gas can reach

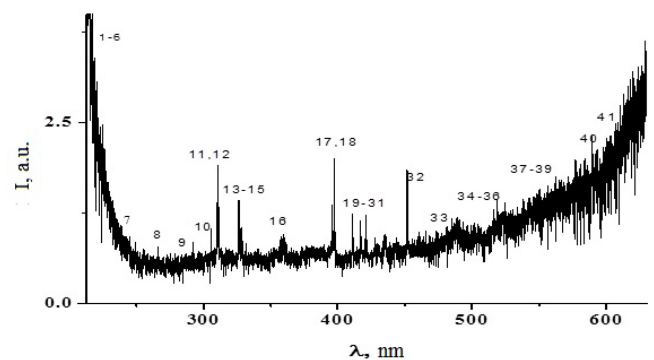


**Figure 6.** The plasma emission spectrum of the overstressed discharge of nanosecond duration between the aluminum and chalcopyrite electrodes at an argon pressure of 101 kPa.

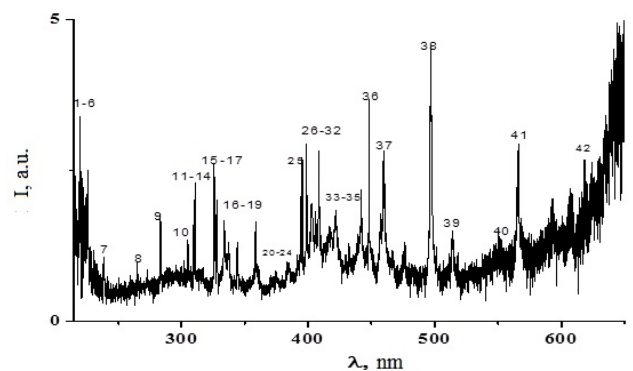


**Figure 7.** The spectrum of plasma emission of the overstressed discharge of nanosecond duration between the aluminum and chalcopyrite electrodes at a nitrogen pressure of 101 kPa.

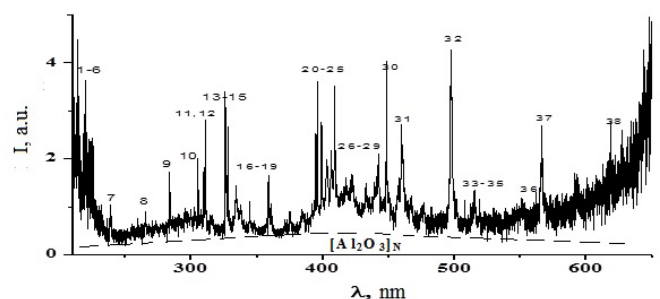


**Figure 8.** Emission spectra of overstressed bipolar nanosecond discharge between aluminum and chalcopyrite electrodes in air at a pressure of 101 kPa.

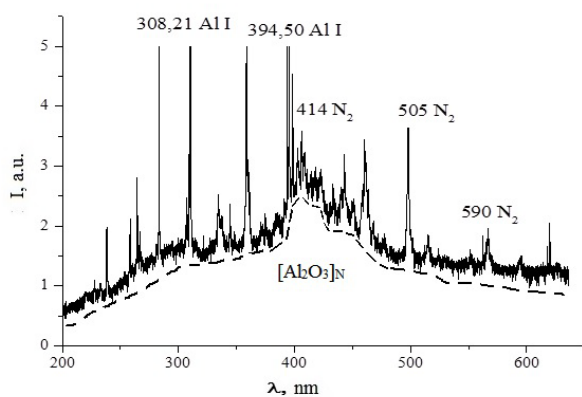


**Figure 9.** Emission spectrum of overstressed discharge of nanosecond duration between aluminum electrodes in a mixture of nitrogen and oxygen (100-1;  $p = 101.3$  kPa); dashed line-  $[Al_2O_3]N$  - designation of alumina nanoparticles.

1016-1017  $cm^{-1}$  [26]. Proceeding from this, the mechanism of the formation of excited metal ions in the studied plasma can be determined by the processes of their excitation by electrons, after which the processes of electron-ion recombination begin. So, for zinc ions, the corresponding effective cross sections of excitation by electrons reach - 10-16  $cm^2$  [27].

On the other hand, proceeding from the peak structure of current pulses, the processes of stepwise excitation and stepwise ionization through the corresponding metastable states typical of high-current high-pressure discharges are also important [28]. Therefore, the probable mechanism for the formation of doubly charged ions of copper, aluminum and argon in the ground energy state can be the excitation of the corresponding singly charged ions by electron impact and the processes of dielectronic recombination of two and singly charged ions with plasma electrons.

### Transmission spectra of synthesized films

The absorption coefficient of UV light by films of ternary chalcopyrite  $CuInSe_2$  is rather large and is in the range (4-6)  $\times 10^5$   $cm^{-1}$  [29]. In the visible and near infrared regions of the spectrum, the absorption coefficient of ternary chalcopyrite decreases to 104  $cm^{-1}$ , and in the wavelength range of 1000-1200 nm it still significantly decreases (to 10  $cm^{-1}$ ). It follows from this, the need to expand the band gap of this semiconductor, and an increase in the absorption coefficient in the infrared region of the spectrum. This can be realized by transforming the  $CuInSe_2$  compound into thin films of quaternary chalcopyrite of the  $CuAlInSe_2$  type.

Typical UV transmission spectra of a deuterium lamp by synthesized thin films, possibly based on the quaternary compound  $CuAlInSe_2$ , in the spectral range 200-500 nm at various nitrogen pressures are shown in Fig.10. The technique and technique of this experiment are given in [30].

The transmission of thin films synthesized from the plasma components of aluminum and ternary chalcopyrite, in comparison with the transmission of the substrate, decreased by 3 - 4 times, and for the film obtained using an overstressed discharge of nanosecond duration in nitrogen it was minimal at atmospheric pressure. The shapes of the transmission

spectra of the films synthesized at nitrogen pressures of 13.3 and 101.3 kPa were similar. The decrease in the transmission of a thin film that was synthesized at atmospheric nitrogen pressure as compared to the transmission of a film obtained at a nitrogen pressure of 13.3 kPa may be due to the smaller film thickness, which was synthesized at a low gas pressure, since the energy contribution to the plasma at atmospheric nitrogen pressure the corresponding contribution prevailed 5.5 times at a nitrogen pressure of 13.3 kPa; therefore, the amount of atomized substance of the electrode material was greater at an atmospheric pressure of nitrogen.

When replacing a gas-discharge broadband ultraviolet lamp with a thermal one, the transmission spectra of the same films were investigated in the wavelength range of 400-800 nm. In this case, too, the main features of the transmission spectra of the synthesized thin films based on the sputtering of ternary chalcopyrite and aluminum at various nitrogen pressures correlated with the above results for the UV spectral range (Figure 10).

Our results for the chalcopyrite plasma correlate with the data for a film deposited from the products of an overstressed discharge of nanosecond duration of atmospheric pressure between aluminum electrodes in a mixture of nitrogen and oxygen, when the deposited material consists of nanostructures of aluminum oxide [31].

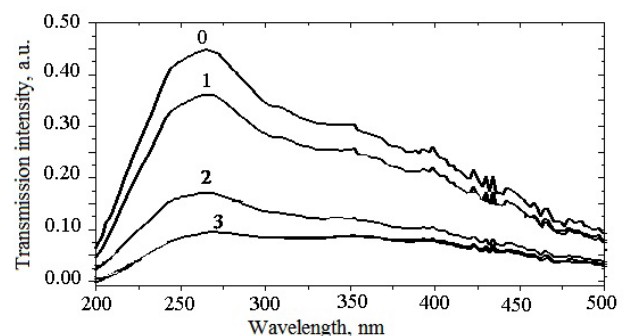


**Figure 10.** Spectra of light transmission by films deposited on quartz substrates, at different pressures of nitrogen in the discharge chamber and when probing them with deuterium lamp radiation: 0 - without sample; 1 - pure quartz glass; 2 - electrodes: one of  $CuInSe_2$ , at a nitrogen pressure of 13.3 kPa; 3 - electrodes: one of  $CuInSe_2$ , the second of aluminum at a nitrogen pressure of 101.3 kPa.

### Conclusions

Thus, the experimental studies of the characteristics of an overvoltage nanosecond discharge showed that between the aluminum and chalcopyrite electrodes in vapor-gas mixtures based on buffer gases of atmospheric pressure Ar,  $N_2$ , or air, a diffuse discharge ignites at the initial moments of time, which is further contracted, as evidenced by the presence of a characteristic spark continuum of radiation in the spectral region of 200-650 nm. The shape of the spark continuum of plasma emission in mixtures with argon differed from the continuum in the medium of oxygen-containing gases, which is due to the radiation of aluminum oxide nanostructures.

**Table 3.** The results of identification of the most intense spectral lines of the aluminum atom and single-charged ion, as well as the molecular bands of the decay products of the chalcopyrite molecule in an overstressed discharge of nanosecond duration ignited at an air pressure of 101.3 kPa.

№	$\lambda_{\text{tabl}}, \text{nm}$	$I_{\text{exp}}, \text{a.u.}$	Object	$E_{\text{low}}, \text{eV}$	$E_{\text{up}}, \text{eV}$	Lower <sub>term</sub>	Upper <sub>term</sub>
1	214.89	4.60	Cu I	1.39	7.18	4s <sup>2</sup> 2D	5f <sup>2</sup> F <sup>o</sup>
2	218.17	3.00	Cu I	0.00	5.68	4s <sup>2</sup> S	4p' <sup>2</sup> P <sup>o</sup>
3	219.56	2.05	Cu II	8.78	14.43	4p <sup>3</sup> D <sup>o</sup>	4d <sup>3</sup> F
4	219.95	3.60	Cu I	1.39	7.02	4s <sup>2</sup> 2D	4p'' <sup>2</sup> D <sup>o</sup>
5	221.45	2.75	Cu I	1.39	6.98	4s <sup>2</sup> 2D	4p'' <sup>2</sup> P <sup>o</sup>
6	225.80	2.30	Al I	0.00	5.49	3p <sup>2</sup> P <sup>o</sup>	7s <sup>2</sup> S
7	239.07	1.00	Al II	13.07	18.26	4p <sup>3</sup> P <sup>o</sup>	10d <sup>3</sup> D
8	261.83	0.88	Cu I	1.39	6.12	4s <sup>2</sup> 2D	5p <sup>2</sup> P <sup>o</sup>
9	284.02	1.75	Al I	4.02	8.39	3d <sup>2</sup> D	3d <sup>2</sup> D <sup>o</sup>
10	306.34	2.00	Cu I	1.64	5.68	4s <sup>2</sup> 2D	4p' <sup>2</sup> P <sup>o</sup>
11	308.21	1.84	Al I	0.00	4.02	3p <sup>2</sup> P <sup>o</sup>	3d <sup>2</sup> D
12	309.27	2.79	Al I	0.01	4.02	3p <sup>2</sup> P <sup>o</sup>	3d <sup>2</sup> D
13	324.75	3.37	Cu I	0	3.82	4s <sup>2</sup> S	4p <sup>2</sup> P <sup>o</sup>
14	327.39	3.10	Cu I	0	3.39	4s <sup>2</sup> S	4p <sup>2</sup> P <sup>o</sup>
15	329.05	2.67	Cu I	5.07	8.84	4p' <sup>4</sup> F <sup>o</sup>	4d' <sup>4</sup> F
16	337.13	1.47	N2	Second positive system C <sup>3</sup> Pu+-B <sup>3</sup> Pg+ (0;0)			
17	344.60	1.10	N2	Second positive system C <sup>3</sup> Pu+-B <sup>3</sup> Pg+ (4;5)			
18	357.69	1.68	N2	Second positive system C <sup>3</sup> Pu+-B <sup>3</sup> Pg+ (0;1)			
19	375.54	0.88	N2	Second positive system C <sup>3</sup> Pu+-B <sup>3</sup> Pg+ (1;3)			
20	394.40	2.49	Al I	0.00	3.14	3p <sup>2</sup> P <sup>o</sup>	4s <sup>2</sup> S
21	396.15	3.63	Al I	0.01	3.14	3p <sup>2</sup> P <sup>o</sup>	4s <sup>2</sup> S
22	402.26	2.77	Cu I	3.79	6.87	4p <sup>2</sup> P <sup>o</sup>	5d <sup>2</sup> D
23	405.67	2.00	Al II	15.47	18.52	3s4d <sup>1</sup> D	3s15p <sup>1</sup> P <sup>o</sup>
24	409.48	0.45	N2	Second positive system C <sup>3</sup> Pu+-B <sup>3</sup> Pg+ (4;8)			
25	410.17	0.37	In I	-	3.02	5s2 <sup>5</sup> p <sup>2</sup> P <sup>o</sup>	5s26s <sup>2</sup> S <sub>1/2</sub>
26	420.05	1.63	N2	Second positive system C <sup>3</sup> Pu+-B <sup>3</sup> Pg+ (2;6)			
27	423.65	1.69	N2	Second positive system C <sup>3</sup> Pu+-B <sup>3</sup> Pg+ (1;2)			
28	434.36	1.52	N2	Second positive system C <sup>3</sup> Pu+-B <sup>3</sup> Pg+ (0;4)			
29	441.67	2.10	N2	Second positive system C <sup>3</sup> Pu+-B <sup>3</sup> Pg+ (3;8)			
30	451.13	4.06	In I	0.27	3.02	5s <sup>2</sup> 5p <sup>2</sup> P <sup>o</sup>	5s <sup>2</sup> 6s <sup>2</sup> S <sub>1/2</sub>
31	459.97	2.73	N2	Second positive system C <sup>3</sup> Pu+-B <sup>3</sup> Pg+ (2;4)			
32	500.51	0.53	N II	25.50	27.97	3s <sup>5</sup> P	3p <sup>5</sup> P <sup>o</sup>
33	510.55	0.46	Cu I	1.39	3.82	4s <sup>2</sup> 2D	4p <sup>2</sup> P <sup>o</sup>
34	515.83	0.51	Cu I	5.69	8.09	4p' <sup>2</sup> P <sup>o</sup>	5s' <sup>2</sup> D
35	521.82	0.58	Cu I	3.82	6.19	4p <sup>2</sup> P <sup>o</sup>	4d <sup>2</sup> D
36	556.69	0.93	Se II				
37	566.66	2.65	N II	18.46	20.65	2s <sup>2</sup> 2p3s <sup>3</sup> P <sup>o</sup>	2s <sup>2</sup> 2p3p <sup>3</sup> D
38	618.86	2.78	Cu II	14.99	16.99	4p'' <sup>1</sup> D <sup>o</sup>	5d <sup>3</sup> F

The maximum pulsed electric power of the discharge in argon was 4 MW (energy contribution to plasma - 423 mJ), in air 3 MW (energy contribution to plasma - 222 mJ), in nitrogen 5 MW (energy contribution to plasma - 410 mJ).

The studies of the spectral characteristics of plasma based on vapor-gas mixtures "argon, nitrogen, air-Aluminum-CuInSe2" showed that the most intense are the spectral lines of the atom and singly charged copper ion in the range 200-

225 nm and the spectral lines of atoms and singly charged aluminum ions in the wavelength range 225-310 nm, as well as lines of the atom of aluminum, indium and copper in the range of the spectrum 310-525 nm. The 618.86 nm CuII line stood out from the ionic lines in the spectrum. All spectral lines of metal atoms and ions, which were components of the electrode material, were observed against the background of a wide band of nanostructures of aluminum oxide. In a discharge based

on buffer gases - nitrogen and air, bright bands of the second positive system of the nitrogen molecule were observed in the UV and visible regions of the spectrum, as well as two intense spectral lines 500.5; 566.6 nm NII.

To diagnose the deposition of films of quaternary chalcopyrite of the  $\text{CuIn}_{1-x}\text{Al}_x\text{Se}_2$  type in real time, the following separately placed intense lines can be used: 307.38 Cu I, 329.05 Cu I, 410.17 In I, 451.13 nm In I, as well as 308.21; 309.27; 394.40; 396.15 nm Al I.

The presence in the plasma emission spectra of the main spectral lines of atoms and singly charged ions of aluminum, copper, and indium allows one to assume the possibility of the deposition of a thin nanostructured film of quaternary chalcopyrite  $\text{CuIn}_{1-x}\text{Al}_x\text{Se}_2$  outside the discharge plasma on the surface of a solid dielectric substrate, as was done for films of ternary chalcopyrite.

The study of the transmission spectra of probing radiation in the wavelength range of 200-800 nm by films based on ternary chalcopyrite and aluminum vapor, which were synthesized by a pulsed gas-discharge method in nitrogen or air, showed that the least transmission is for films that were synthesized at atmospheric pressure of gases; it is likely that the thin film obtained from the degradation products of electrodes belongs to the quaternary chalcopyrite  $\text{CuAlInSe}_2$ .

The authors are grateful to O.I. Mini. and Z.T. Gomoki for help in conducting experiments and R.V. Hrytsak for help in processing the experimental results.

## References

1. Tarasenko VF. Runaway electrons preionized diffuse discharge. Nova Science Publishers Inc., New York. 2014.
2. Shuaibov O, Minya O, Chuchman M, et al. Parameters of Nanosecond Overvoltage Discharge Plasma in a Narrow Air Gap between the Electrodes Containing Electrode Material Vapor. Ukr J Phys. 2018;63:790.
3. Shuaibov AK, Minya AI, Malinina AA, Gritsak RV, Malinin AN. Characteristics of the nanosecond overvoltage discharge between  $\text{CuInSe}_2$  chalcopyrite electrodes in oxygen - free gas media, Ukr J Phys. 2020; 65(5):400.
4. Vons VA, de Smet LCPM, Munao D, et al. Silikon nanoparticles produced by spark discharge, J Nanopart Res. 2011;13:4867.
5. Itina TE, Voloshko A. Nanoparticle formation by laser ablation in air and by spark discharge at atmospheric pressure. Appl Phys B. 2013; 113: 473-478.
6. Pai DZ, Kumar S, Levehenko I, Lacoste DA, Laux CO, Ostrikov K. Nanomaterials synthesis in air atmospheric pressure using nanosecond repetitively pulsed spark discharges. Abstract for the 6th International Workshop on Microplasmas, Paris, April 3-6, 2011, P.77.
7. Ivanov VV, Efimov AA, Mylnikov DA, et al. Letters to ZhTF. 2016;42(16):95.
8. Ampylov AM, Barxudarov EM, Kozlov YN, et al. UV radiation of a high-voltage multi-electrode surface discharge in a gas environment. Plasma Physics. 2019;45(3):268.
9. Shuaibov AK, Minya AY, Gomoki ZT, et al. Plazma Reactor generating synchronous Flows of bactericidal UV Radiation and Nanostructures of Zinc, Copper, Iron Oxides and Chalcopyrite. HSOA Journal of Biotech Research & Biochemistry. 2020;3(1):100005.
10. Axmadeev VV, Vasylyak LM, Kostyuchenko SV, Kudryavcev NN, Kurkyn GA. Spark breakdown of air by nanosecond voltage pulses. Journal of technical physics. 1996;66(4):58.
11. Beloplotov DV, Tarasenko VF, Lomaev MY. Luminescence of aluminum atoms and ions in a repetitively pulsed nanosecond discharge initiated by runaway electrons in nitrogen. Optics of atmosphere and ocean. 2016;29(2):96.
12. Beloplotov DV, Lomaev VI, Sorokin DA, Tarasenko VF. Blue and green jets in laboratory discharges initiated by runaway electrons. Journal of Physics : Conference Series. 2015; 652:012012.
13. Beloplotov DV, Lomaev MY, Tarasenko VF. On the nature of emission of blue and green jets in laboratory discharges initiated by a beam of runaway electrons, Optics of atmosphere and ocean. 2015; 28(4):349.
14. Mesyats GA. Ecton or electron avalanche from metal. Usp Fizich Nauk. 1995;38:567.
15. Lopez-Garcia J, Placidi M, Fontane X, et al.  $\text{CuIn}_{1-x}\text{Al}_x\text{Se}_2$  thin film solar cells with depth gradient compositions prepared by selenization of evaporated metallic precursors. Solar Energy Materials & Solar Cells evaporated. 2015;132:245.
16. Kostyrya YD, Tarasenko VF, Rybka DV. Features of registration of runaway electrons during breakdown of air at atmospheric pressure by voltage pulses with a leading edge of 0.5  $\mu\text{s}$ . Proceedings of higher educational institutions. Physics. 2014;57(12/2):220.
17. NIST Atomic Spectra Database Lines Form [https://physics.nist.gov/PhysRefData/ASD/lines\\_form.html](https://physics.nist.gov/PhysRefData/ASD/lines_form.html)
18. Pyrs R, Gejdon A. Identification of molecular spectra. Moskva: Publishing house YL: 1949.
19. Kacher YE, Shuaibov AK, Rygan MY, Dashhenko AY. Optical diagnostics of laser evaporation of the polycrystalline compound  $\text{CuInS}_2$ . High temperature, 2002; 40(6):880.
20. Shuaibov AK, Minya AY, Gomoki ZT, et al. Characteristics and Parameters of Overstressed Nanosecond Discharge Plasma between Electrodes from Chalcopyrite ( $\text{CuInSe}_2$ ) in Argon at atmospheric Pressure. Surface Engineering and Applied Electrochemistry. 2020;56(4):474.
21. Kortov VS, Ermakov AE, Zacepyn AF, Uajt MA, Nykyforov SV. Features of the luminescent properties of nanostructured aluminum oxide. Solid state physics. 2008;50( 5):916.
22. Gasenkova YV, Muxurov NY, Vaxyox YM. Optical properties of anodized aluminum substrates as a basis for threshold detectors, Reports of BGUYR. 2016;96(2): 114.
23. Van der Horst RM, Verreycken T, Van Veldhuizen EM, Bruggerman PJ. Yime-resolved optical emission spectroscopy of nanosecond pulsed discharges in atmospheric-pressure  $\text{N}_2$  and  $\text{N}_2/\text{H}_2\text{O}$  mixtures. J Phys D: Appl Phys. 2012;45:345201.
24. Levko D, Raja LL. Early stage time evolution of a dense nanosecond microdischarge use in fast switching applications. Physics of Plasmas. 2016;22:123518.
25. Gomonai AN. Radiative Decay  $\text{np}_2$  autoionization States under dielectronic Recombination of the  $\text{Zn}^+$  and  $\text{Cd}^+$  Ions. Journal of Applied Spectroscopy. 2015;82(1):17.
26. Shyker R, Binur Y, Szoke A. Studies of afterglows in noble-gas mixtures. A model for energy transfer in He/Xe. Phys Rev A. 1975;12(2):512.
27. Novykov GF, Gapanovych MV. Solar converters of the third generation based on Cu-In-Ga- (S, Se). Physics-Uspekh. 2017; 187(2):173.
28. Minya OJ, Krasylynecz VM, Shuaibov OK, et al. Transmission spectra of thin nanostructured films based on copper, aluminum and chalcopyrite obtained by pulsed gas discharge method. Uzhhorod University Scientific Herald Series Physics. 2019;46:84.
29. Shuaibov A, Minya A, Malinina A, et al. Study of the Formation Conditions of Aluminum Oxide Nanoparticles in an Overstressed Nanosecond Discharge Between Aluminum Electrodes in a Mixture of Nitrogen and Oxygen. Journal of Metallic Material Research. 2020;3(2):37.